Molecular dynamics simulation of water from 10 to 1273 K

M. W. Evans,[a] G. C. Lie, and E. Clementi
IBM Corporation, Data Systems Division, Dept. 48B/MS 428, Neighborhood Road, Kingston, New York 12401

(Received 30 October 1987; accepted 7 January 1988)

The molecular dynamics of liquid water have been simulated over a wide range of thermodynamic conditions using a five by five site–site model for the intermolecular potential recently developed by Evans. The model reproduces the pressure satisfactorily for temperatures up to 1273 K at constant density of 1 g/cm^3. Within the uncertainty, the experimental pressure is also reproduced satisfactorily at the critical point. Two simulations at 773 and 1043 K have also been carried out at constant molar volume of 8.5 cm^3/mol. The molecular dynamics of the sample were investigated at each state point with a range of auto- and cross-correlation functions. Some of these have been computed at constant molar volume over a 15 kbar range of pressure and 1000 K range of temperature. They suggest that diffusional dynamics in liquid water are largely determined by density. Some results at 10 (1 bar) and 77 K (1 bar) were obtained by "splat quenching" at constant molar volume. The oxygen–oxygen pair distribution functions from these simulations have been compared with the results available from amorphous solid water at these temperatures.

I. INTRODUCTION

The thermodynamic properties of liquid and amorphous solid water are known experimentally[1-5] from well below room temperature at 1 bar (supercooled) to 250 kbar and 1043 K. The critical point is also known accurately from several different experimental sources in the literature.[6] Therefore, there are sufficient data for the investigation of the liquid state dynamics by computer simulation over a range of state points. It is particularly interesting in this context to compute time correlation functions at constant molar volume at several different state points generated by varying the pressure and temperature. In this context data are available in the literature at a constant density of 1.0 g/cm^3 from 293 K, 1 bar to 1273 K, 15.0 kbar in the liquid state. In this paper simulations are reported along the constant density curve at these state points and at four intermediate points: (1) 373 K, 1.0 kbar; (2) 473 K, 3.0 kbar; (3) 673 K, 7.5 kbar; (4) 773 K, 9.5 kbar, all at a liquid density of 1.0 g/cm^3. At these state points the molar volume is, therefore, constant at 18.0 cm^3/mol. Additionally, experimental data are available from shock wave experiments[4] at a constant inverse density of 0.47 cm^3/g at two state points: (1) 773 K, 230 kbar; (2) 1043 K, 250 kbar, and these provide a further opportunity for simulations at very high pressure and constant molar volume with which to investigate the nature of the molecular dynamics of liquid water through a wide variety of time correlation functions now available.[7-10]

At the critical point of water (647.02 K, 220.91 bar) the experimentally measured critical molar volume is 56.8 cm^3/mol, and simulations at the critical point are reported in this paper of time correlation functions at the fundamental single molecule level. Finally simulations are reported in ultralow temperature conditions at 1.0 bar, 10 K and 1.0 bar, 77 K, in order to compare with the experimental data available[11-14] at these temperatures on amorphous solid ice, high and low density forms, respectively, whose measured densities at 1.0 bar are 1.1 and 0.94 g/cm^3. The low temperature configurations were obtained by suddenly dropping the input temperature at constant molar volume and reequilibrating in the new low temperature configurations. This technique is sometimes known in the literature as "splat quenching" and is equivalent to removing kinetic energy almost instantaneously from the system. This does not result in a phase change, and the configuration in which the system finally equilibrates at low temperature in the computer simulation is amorphous in the sense that it has no regular ice-like structure. The simulations of splat-quenched water appear liquid-like since the time correlation functions at the single molecule level are typical of those for a liquid. If the rate of cooling is very rapid, as in computer simulation, then the structure of the configuration prior to quenching will be retained at the ultralow temperature,[15] frozen into a vitreous condition that is not fluid. This paper attempts to investigate whether this state of matter bears resemblance to the amorphous solid state of ice known experimentally.

The simulations are carried out with a pair potential devised by Evans in previous work,[16] and based on an atom–atom representation of the effective pair potential of water. The hydrogen bonding is mimicked with partial charges at the hydrogen sites and at the lone pair sites, with a zero charge on the oxygen. The performance of this potential has been tested in the literature[17,18] against radiation diffraction data on the liquid structure at 1 bar and room temperature. In this respect it compares favorably with the MCY and ST2 potentials.[19,20] Recently,[21] the Evans and MCYL (flexible water)[22] potentials have been carefully compared through time cross-correlation functions in the laboratory (x,y,z) and moving (1,2,3) frames of reference and found to behave similarly as regard the molecular dynamics in liquid water at room temperature and pressure. However, the Evans potential has not yet been tested experimentally against the var-

[a] Present address: Department of Physics, University College of Swansea, Singleton Park, Swansea SA2 8PP, Wales, United Kingdom and Visiting Academic, Dept. of Microelectronics & Electrical Engineering, Trinity, Collwgw Dublin 2, Republic of Ireland.

 0021-9606/88/085157-09$02.10

ious known ice structures, using the methods developed recently by Morse and Rice.[23] In this paper it is found to reproduce the experimental pressure satisfactorily at a variety of state points mentioned already, i.e., over a thousand degrees of temperature and 250 kbar of pressure.

II. COMPUTER SIMULATION METHODS

The standard methods of constant volume molecular dynamics computer simulation were implemented through the algorithm TETRA, fully described elsewhere.[24,25] This is a code based on the Verlet method for interation of the linear dynamics and computes the net molecular torque from the individual atom–atom forces. The angular momentum is then found by numerical integration of the torque. The systems investigated here all consist of 108 water molecules enclosed in a cubic box with periodic boundary conditions.

At each state point the time correlation functions were computed over 6000 time steps of 0.5 fs each dumped every second record into 3000 configurations. At each state point the algorithm computes the mean pressure over 6000 time steps at input temperature and molar volume. The simulated mean pressure was then compared with the measured pressure and reported in Table I. This procedure was repeated at several different state points in order to determine the thermodynamics from the given pair potential for effective water–water interactions.

The effective intermolecular pair potential is described fully in the literature. It is based on a three by three atom–atom Lennard-Jones model of the hydrogen–hydrogen, hydrogen–oxygen, and oxygen–oxygen interactions, supplemented by positive partial charges on the hydrogens and negative partial charges on the lone pair sites. In previous work the pressure computed from the program was adjusted to 1 bar at 293 K for an input molar volume of 18.0 cm^3/mol.[16] In the simulations reported here the model parameters optimized by this procedure were retained unchanged at each state point for consistency of interpretation.

III. SLAM AND SPLAT QUENCHING

The experimental techniques of slam and splat quenching were mimicked in this work by very simply dropping the temperature instantaneously, holding constant the input molar volume. For the experimentally observed[11–14] input molar volume at 10 K the resulting computed pressure was observed to be negative, indicating that the "frozen" configuration was in a state of metastable equilibrium, the molar volume being too high to sustain true thermodynamic equilibrium, and the computed temperature tended to drift upwards from the input temperature of the algorithm. It is difficult to deduce whether such a state is vitreous or supercooled liquid, and the results presented below in terms of time correlation functions are meant to resolve this question in dynamical terms. Atom–atom pair distribution functions (PDF) were also computed in the metastable equilibrium condition for comparison with the experimental data available for the oxygen–oxygen PDFs in the amorphous solid state of water mentioned already, whose density at 10 K is approximately the same as that of liquid water at room temperature and pressure. From a recent review work of Angell,[15] however, it seems that the extrapolated density of liquid water supercooled to 10 K must be far higher, and the molar volume correspondingly lower. From these considerations it seems that the state attained in the computer simulation by splat quenching to 10 K at about the same molar volume as occupied by liquid water at room temperature is structurewise akin to amorphous solid water. Further tests of this hypothesis are reported below. Adjustment of the input molar volume at 10 K from 18.0 to 13.75 cm^3/mol raised the computed pressure to approximately 1 bar but this had little effect on the observed molecular dynamics.

TABLE I. Comparison of experimental pressures and computed pressures calculated from the Evans potential.

Input temperature (K)	Input molar vol (cm^3/mol)	Computed mean presure (bar)	Measured pressure (bar)
293	18.0	-137 ± 300	1.0
373	18.0	1515 ± 500	1 000.0
473	18.0	3693 ± 800	3 000.0
673	18.0	8773 ± 950	7 500.0
773	18.0	11200 ± 1000	9 500.0
1273	18.0	19132 ± 1800	15 000.0
773	8.5	521640 ± 30000	230 000.0
1043	8.5	559670 ± 40000	250 000.0
647	56.8	300 ± 250	220.9

IV. RESULTS AND DISCUSSION

The computed mean pressures over 6000 time steps are reported in Table I, and compared with the experimental equivalents at the same state points. Omitted from this table are the results at 10 and 77 K, because the computed pressures are negative as discussed already. The overall agreement in Table I is satisfactory, and well within the limits of uncertainty of the computer simulation method. This is evidence in favor of the model pair potential, but a closer examination of its behavior in the ices[23] will probably reveal shortcomings which would have to be remedied by further refinement of the model parameters. This will be the subject of future work.

The table shows that the computed pressures tend to increase more steeply than the observed pressures as the temperature rises from 293 to 1273 K at constant molar volume. The pressure at the critical point is, however, reproduced satisfactorily, and the agreement with the observed pressure is within the uncertainty at the input critical molar volume at 56.8 cm^3/mol. At the great pressures observed in liquid water under high temperature conditions induced by shock waves[1–5] the potential produces a computed pressure about twice the observed value in the case of worst disagreement at the 250 kbar state point. In constant volume computer simulation a slight change of box size (input molar volume at constant temperature) has a very big effect on the computed pressure, and in view of this the broad range of agreement between computed and observed liquid pressures in Table I has to be regarded as satisfactory until the poten-

tial is fully tested out against the ice structures using the methods of Morse and Rice.[23]

A. The molecular dynamics

A language of molecular dynamics is that of time correlation functions, and these are used extensively in this section to monitor the liquid dynamical behavior from 10 to 1273 K over 250 kbar of liquid pressure. The technical difficulties of achieving this experimentally are formidable, even at pressures into the kbar range. Apart from the thermodynamic data in Table I, little has been achieved experimentally in this area. Computer simulation therefore provides a fairly precise alternative to actual data on the molecular dynamics of liquid water over its complete range of existence. In some cases the simulation provides valuable insight to the nature of rotational and translational diffusion in liquid water which can be obtained in no other way, and which is fundamental to the understanding of molecular diffusion processes in general. This insight is achieved, for example, in terms of cross-correlation functions (CCF) of different kinds, which signal the complete inapplicability of "classical" diffusion theory[24] in liquid water. For example, we illustrate in Fig. 1 the direct statistical cross correlation between the molecular center of mass velocity v and the time derivative of the molecular dipole vector μ,

$$C_1^{ij}(t) = \frac{\langle v_i(t)\dot{\mu}_j(0)\rangle}{\langle v_i^2(0)\rangle^{1/2}\langle \dot{\mu}_j^2(0)\rangle^{1/2}}$$

in the laboratory frame of reference (x,y,z) for the various state points. It is clear from these results that the intensity of the direct correlation becomes greater as the molar volume decreases, and is approximately constant at constant molar volume. The classical theory of dielectric and far infrared spectroscopy[24] takes no account of direct statistical correlation of this nature between translational and orientational dynamics, and provides much less information than computer simulation. Simply put, it is impossible for a water molecule to diffuse in its aqueous environment according to the rules of rotational or translation diffusion theory. Furthermore, the language of cross-correlation function as illustrated in Fig. 1 seems simpler than that of hydrogen bond breaking and reformation. What little is known experimentally about the diffusion of water molecules seems to be interpreted vaguely in terms of the dynamics of H bonds. The large number of cross-correlation functions now known provide a clearer and more precise alternative description through the intermediacy of computer simulation. Furthermore, the trajectories and configuration generated in the simulation can be used self-consistently for comparison with experimental data as in Table I and also to generate a range of autocorrelation functions (ACF) which are Fourier transform signatures of various measurable spectral band shapes.[24]

The behavior of these ACFs over the complete range of existence of liquid water is not known experimentally, because of the obvious technical difficulties. At constant density the effect on the orientational autocorrelation function of increasing the pressure and the temperature is to increase the rate of decay of the ACF up to about 9.5 kbar and 773 K, and therefore to decrease the correlation time. At about 15 kbar and 1273 K the orientational ACF develops a long tail,

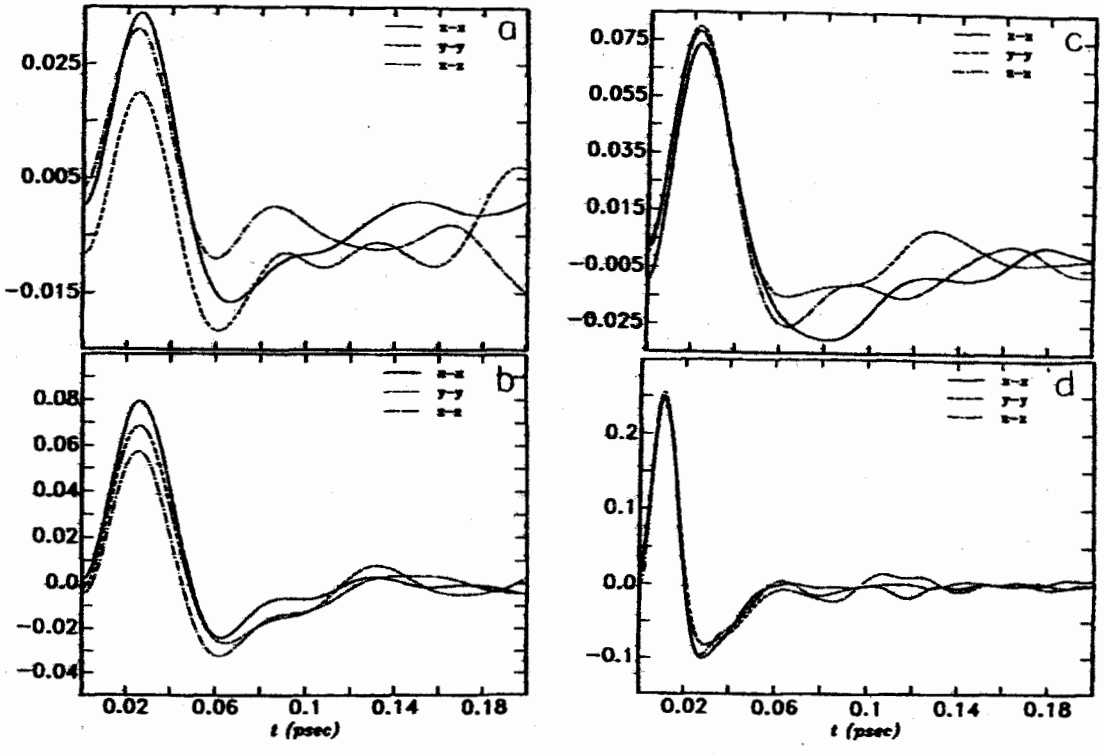

FIG. 1. Diagonal elements of the "coupling function" $C_1^{ij}(t)$ for liquid and compressed gaseous water with: (a) molar volume 1800 cm^3/mol, pressure 20 bar, at 293 K (steam); (b) 18.0 cm^3/mol, 1 bar, 293 K; (c) 18.0 cm^3/mol, 15 kbar, 1273 K; (d) 8.5 cm^3/mol, 250 kbar, 1043 K.

indicative of an initial rapid decay followed by a much slower diffusional type of time dependence. At 250 kbar and 1043 K in the very dense liquid state at half the molar volume the orientational correlation function has about the same characteristics, but its correlation time is longer. The longest and the shortest correlation times are found, respectively, in the splat quenched sample at 10 K and at the critical point. The behavior of this correlation function approximately reflects that of the dielectric relaxation time, but not exactly, because the latter has contributions from cross correlations between molecules in any condensed state of matter. At present, dielectric relaxation measurements seem to be unavailable at most state points simulated in this paper, but are given elsewhere[25] at 1 bar down to low temperatures.

In this work we have also computed the time dependence of the rotational velocity autocorrelation function (RVACF) as a function of density, pressure, and temperature. The oscillations in the RVACF gradually damp out as the pressure and temperature is increased at constant molar volume, so that the cage effect (torsional oscillation) is gradually lost as the kinetic energy is increased, even at constant volume. At 250 kbar, 1043 K the oscillations are deepened and occur at much shorter times, due to the high density of liquid water at these ultrahigh pressures and temperatures.[1-5] The rotational velocity ACF splat quenched to 10 K is almost identical to its equivalent at 1 bar, 293 K, and this is due to the fact that the high density dynamics are frozen in by the technique of splat quenching to 10 K. In contrast, the rotational velocity ACF at the critical point is free of oscillations, indicating that the molecular motion is fairly free from interrupting by collisions. Even at the critical point, however, Fig. 1 shows that the linear center of mass velocity is strongly correlated to the rotational velocity direct in the laboratory frame of reference. In fact, even in pressurized steam at a molar volume of 1800 cm^3/mol [Fig. 1(a)] there is residual cross correlation of this type, and this clearly means that the available theories of collision line broadening[24] have to be revised in line with this finding. The rotational velocity ACF is the Fourier transform, essentially speaking, of the far infrared power absorption coefficient,[24] the frequency dependence of which contains direct information on the rotational velocity ACF and indirect information on the cross correlations of Fig. 1.

The autocorrelation function of the center of mass molecular linear velocity develops a negative overshoot at high liquid density (at 250 kbar), but is otherwise a monotonic decay over the 0.1 ps range. The correlation time is longest at the critical point, and in the splat quenched condition at 10 K the ACF is almost identical in time dependence to its counterpart at 296 K and 1 bar, despite the great difference in kinetic energy. This seems to imply that the dynamics are driven by density rather than kinetic energy, i.e., the dependence of the time ACFs on density is much greater than on kinetic energy (or temperature). In this respect, therefore, the much sharper negative overshoot observed in the velocity ACF with the MCYL potential in the liquid state at 1.0 bar is probably due to the 8000 bar of pressure generated by the potential at that temperature and at an input molar volume of 18.0 cm^3/mol.[22]

We have also computed the angular velocity ACF over the same range of state points. While exhibiting broadly similar behavior to the rotational velocity ACFs the negative overshoot in the angular velocity ACF is lost at 15 kbar and 1273 K, and the oscillatory nature is lost at the critical point. This ACF is at its most oscillatory, however, in the high density liquid at 250 kbar, with a negative overshoot of about 0.3. Again it is interesting to observe that the behavior at 10 K in the splat quenched condition is nearly identical to that at room temperature.

B. The moving frame of reference

If a frame of reference is defined with respect to the principal moment of inertia axes of the water molecule as in Ref. 16 then there appear in this frame (1,2,3) cross-correlation functions directly between the molecular linear velocity v and the molecular angular velocity ω. The CCF is usually normalized as

$$C_2^{ij}(t) = \frac{\langle v_i(t)\omega_j(0)\rangle}{\langle v_i^2\rangle^{1/2}\langle \omega_j^2\rangle^{1/2}}$$

and in liquid water the (2,3) and (3,2) elements exist and are symmetry allowed. The dependence of these elements on density, pressure, and temperature is illustrated in Fig. 2. At a constant molar volume of 18.0 cm^3/mol (see Table I), but different temperatures and pressures, the two elements remain constant relative to each other and also in time dependence and intensity. They are not mirror images because of lack of symmetry in the water molecule itself. As for the direct laboratory frame cross correlations of Fig. 1 then, the moving frame CCF $C_2^{ij}(t)$ is also driven primarily by density, not by kinetic energy. At constant density (i.e., molar volume) the CCF characteristics remain constant. However, if the density of the liquid is changed, e.g., doubled by the application of 250 kbar of pressure at 1043 K, then the intensity of the (2,3) and (3,2) elements is each increased by roughly four times. In very dense liquid water, therefore, the laboratory frame (Fig. 1) and moving frame (Fig. 2) cross correlations are very strong, signaling the onset of solid-like behavior at very high density. In the molecular crystal it is quite clear what statistical cross correlations of the type shown in Figs. 1 and 2 mean. They are signatures of roto-translational lattice modes at the single molecule level. In the liquid state they are the remnants of lattice-like behavior. In Fig. 2 it is also shown that the moving frame CCF in the splat quenched condition at 10 K again remains very similar in time dependence to its counterpart at 296 K and 1 bar. Finally the intensity of the CCF decreases at the critical point, but its time dependence remains remarkably constant. This remains true at an additional state point incorporated in this figure for steam, where the molar volume is 1800 cm^3/mol and the computed pressure 20 bar at 293 K.

C. Theory of cross-correlation functions of Fig. 1

In this section a general simple theory is developed for the cross-correlation function observed in Fig. 1 between the molecular linear center of mass velocity and the rotational velocity. This is a simple theory based on the idea of linked

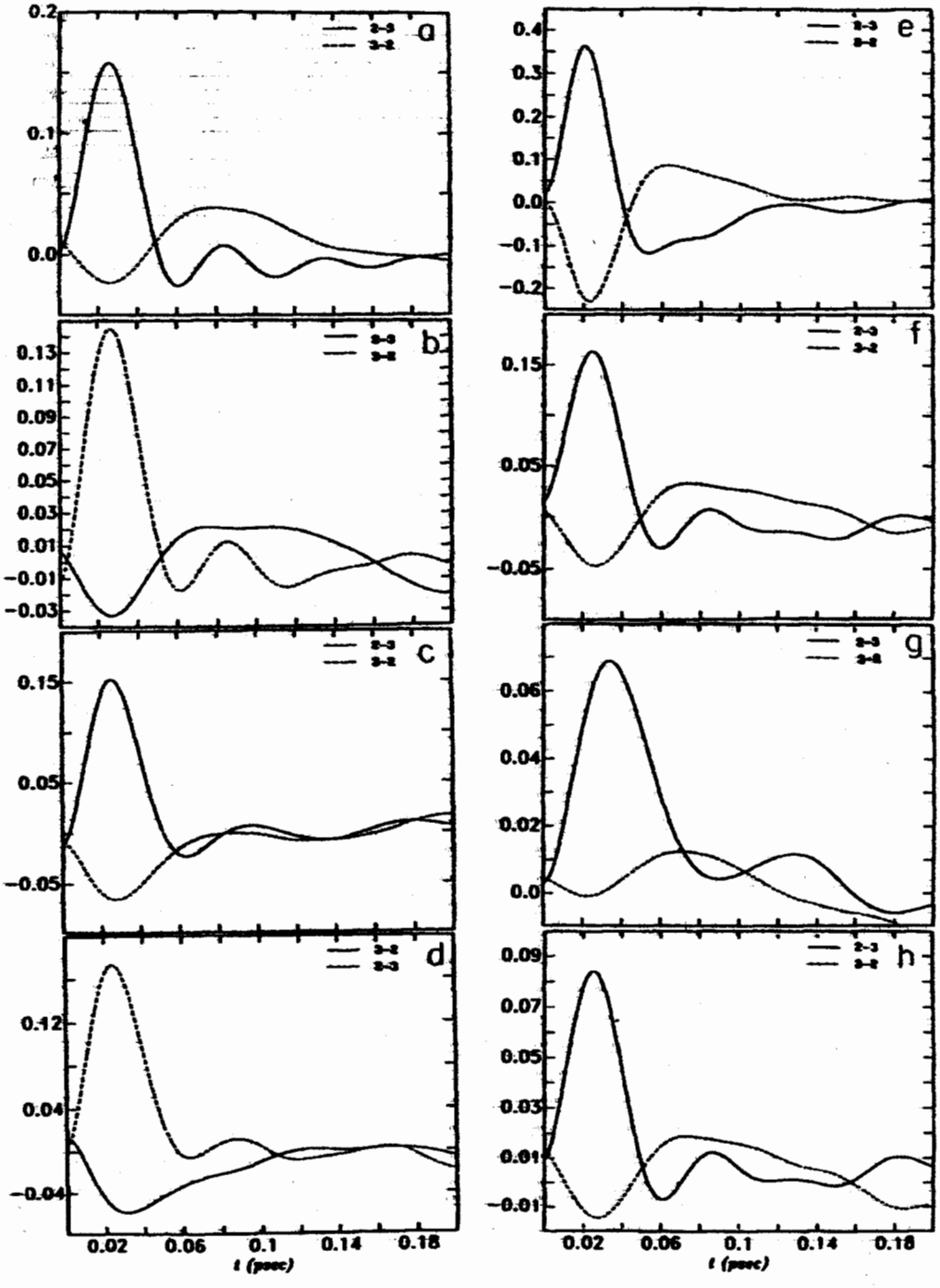

FIG. 2. (2,3) and (3,2) elements of the moving frame cross-correlation matrix $C_2^t(t)$ for liquid and compressed gaseous water at: (a) molar volume 1800 cm^3/mol, pressure 1 bar, 293 K (steam); (b) 18.0 cm^3/mol, 1 bar, 373 K; (c) 18.0 cm^3/mol, 9.5 kbar, 773 K; (d) 18.0 cm^3/mol, 15 kbar, 1273 K; (e) 8.5 cm^3/mol, 250 kbar, 1043 K; (f) 18.0 cm^3/mol, 1.0 kbar, 10 K; (g) 56.8 cm^3/mol, 221 kbar, 647 K (critical point); (h) 1800 cm^3/mol, 20.0 bar, 293 K (compressed gaseous water).

Langevin equations first proposed by Condiff and Dahler[26] for cross correlation between $\mathbf{v}$ and the molecular angular velocity $\boldsymbol{\omega}$. However, there is no direct laboratory frame cross correlation between $\boldsymbol{\omega}$ and $\mathbf{v}$ because of general symmetry rules generated by parity inversion. To see this type of cross correlation one must use the moving frame as described above.

We first note the kinematic equation

$$\dot{\boldsymbol{\mu}} = \boldsymbol{\omega} \times \boldsymbol{\mu} \tag{1}$$

in the laboratory frame (x,y,z) with origin at the molecular center. This is generally true for any rigid rotating body. The total velocity of an atom in the water molecular is then given by (neglecting vibration):

$$\mathbf{v}_a = \mathbf{v} + \tfrac{1}{2}\boldsymbol{\omega} \times \boldsymbol{\mu}. \tag{2}$$

Thus,

$$\langle \mathbf{v}_a(t) \cdot \mathbf{v}_a(0) \rangle = \langle \mathbf{v}(t) \cdot \mathbf{v}(0) \rangle + \langle \mathbf{v}(t) \cdot \dot{\boldsymbol{\mu}}(0) \rangle + \tfrac{1}{4} \langle \boldsymbol{\mu}(t) \cdot \boldsymbol{\mu}(0) \boldsymbol{\omega}(t) \cdot \boldsymbol{\omega}(0) \rangle. \tag{3}$$

The central term on the right-hand side of this equation denotes the effect of rotation–translation coupling and has been observed for the first time in this work.

The problem is to devise suitable linked Langevin equations for this "coupling term," which appears in all molecu-

lar liquids. It is assumed, therefore, that the rotational velocity, being a fluctuating variable with the units of velocity, is itself driven by a Langevin equation which is in turn linked with the Langevin equation for the center-of-mass linear velocity $\mathbf{v}$. The two equations are linked with cross terms in the manner of Condiff and Dahler,[26] and are written directly in the laboratory frame of reference. In order to simplify the mathematical analysis the cross terms of the Euler equation underlying the rotational dynamics of the vector $\boldsymbol{\mu}$ are neglected, so that the asymmetric top is approximated kinematically by the spherical top with embedded dipole. This is also an approximation used implicitly in the original work of Condiff and Dahler.

The system of linked Langevin equations is then

$$\dot{\mathbf{v}} = \lambda_t \mathbf{v} - \lambda_{tr} \dot{\boldsymbol{\mu}} + \mathbf{F}, \tag{4}$$

$$\dot{\boldsymbol{\mu}} = -\lambda_r \dot{\boldsymbol{\mu}} - \lambda_{rt} \mathbf{v} + \mathbf{N}, \tag{5}$$

where λ_t is the translation friction coefficient, λ_r the rotational friction coefficient, and

$$\lambda_{tr} = -\lambda_{rt}$$

are cross terms. The equations are completed by the stochastic accelerations $\mathbf{F}$ and $\mathbf{N}$.

The linked Langevin equations can be solved by Laplace transformation to give

$$\langle \mathbf{v}(t)\cdot\mathbf{v}(0)\rangle = \frac{\langle v^2(0)\rangle e^{-bt}\{\cos[(c-b^2)^{1/2}t] + (\lambda_r - b)\sin[(c-b^2)^{1/2}t]\}}{(c-b^2)^{1/2}} \quad (c>b^2);$$

$$= \frac{\langle v^2(0)\rangle e^{-bt}\{\cosh[(b^2-c)^{1/2}t] + (\lambda_r - b)\sinh[(b^2-c)^{1/2}t]\}}{(b^2-c)^{1/2}} \quad (c<b^2);$$

with a similar expression for the rotational velocity ACF, the cross-correlation function being given by

$$\langle \mathbf{v}(t)\cdot\dot{\boldsymbol{\mu}}(0)\rangle = \frac{\langle v_i^2(0)\rangle^{1/2}\langle \dot{\mu}_j^2(0)\rangle^{1/2}\lambda_{tr} e^{-bt}\sin[(c-b^2)^{1/2}t]}{(c-b^2)^{1/2}} \quad (c<b^2),$$

where the sine is to be replaced by sinh when the argument is negative.

Here

$$b = 2(\lambda_t + \lambda_r); \quad c = \lambda_t\lambda_r - \lambda_{tr}\lambda_{rt}.$$

Note that the cross-correlation function $\langle \mathbf{v}(t)\cdot\boldsymbol{\mu}(0)\rangle$ can be obtained by integration and the theory provides a number of correlation functions self-consistently in terms of the friction coefficients.

By using far infrared data for the rotational velocity ACF, tracer diffusion analysis for the linear center-of-mass velocity ACF and computer simulation for the cross-correlation function, the three friction coefficients can be defined uniquely. This provides a method of interrelating theory, computer simulation, and experimental data. Alternatively, the theory can be used to parametrize computer simulation results for the velocity, rotational velocity, and cross-correlation function in terms of the friction coefficients. For liquid water computer simulation data at 1 bar, 293 K the three friction coefficients $\lambda_t = 1.0$ THz, $\lambda_r = 25.0$ THz, and $\lambda_{tr} = 50.0$ THz give the curves of Fig. 3 which broadly reflect the computer simulation results theoretically. Nothing more can be expected for a simplified theory, which does not use memory functions to account for the known dependence of friction coefficients on frequency.[25]

It is concluded, therefore, that the the use of a Langevin equation direct for the rotational velocity is justified by the theoretical results of Fig. 2, which give the same pattern of time dependence as the correlation functions simulated in this paper. In the absence of cross correlations, however, a Langevin equation in the rotational velocity is not justifiable because its solution is a simple exponential which does not reproduce the negative overshoot characteristic of all rotational velocity autocorrelation functions in molecular liquids. Similarly the center-of-mass linear velocity ACF often has the well-known negative tail which is not described by a simple Langevin equation in v. It is significant that the linked Langevin equations (4) and (5) produce negative tails both in the velocity and rotational velocity ACFs without invoking the memory functions, and also reproduce the main features of the cross-correlation function between these variable direct in the laboratory frame of reference. The shortcomings of the simple linked Langevin theory can be seen at very short times, because the correlation functions go to zero with a finite slope, due to the fact that the friction coefficients are zero order memory functions with no time dependence. Unfortunately, the introduction of such a time

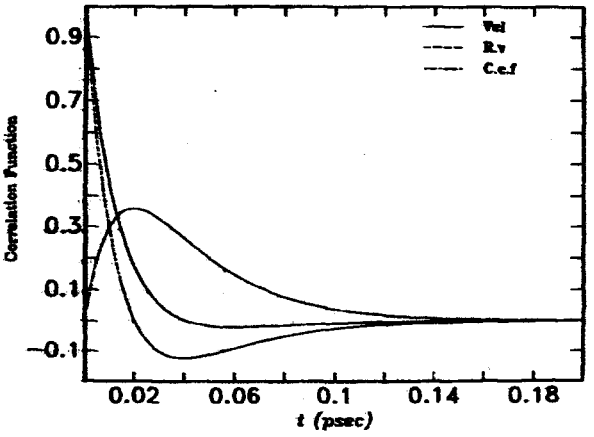

FIG. 3. Theoretical results from the linked Langevin theory: Vel (velocity autocorrelation function), R.v (rotational velocity autocorrelation function), and C.c.f (cross-correlation function). See the text for the parameters used.

dependence would result in an overparametrized theory and the linked Langevin equations would no longer have a simple analytical solution. Similarly the use of the full Euler–Langevin system of linked equations would be self-defeating, because of mathematical intractability. The use of linked Langevin equations between linear and angular velocity is meaningless in the laboratory frame because the cross-correlation function vanishes for all t. Therefore, the system of Eqs. (4) and (5) steers a course between all these obstacles, and seems to be justified by the results.

D. Higher order cross-correlation functions

Recent computer simulation work has uncovered[27–30] the existence of numerous higher order cross-correlation functions in the laboratory frame (x,y,z) and moving frame (1,2,3). In this section we report that we have simulated the various types of cross-correlation function in liquid water over its complete range of existence. The results are too numerous to illustrate in detail, but copies are available on request.

In the moving frame (1,2,3) the diagonal elements of the cross-correlation functions

$$C_3^{ij}(t)=\frac{\langle[\mathbf{v}(t)\times\boldsymbol{\omega}(t)]_i v_j(0)\rangle}{\langle(\mathbf{v}\times\boldsymbol{\omega})_i^2\rangle^{1/2}\langle v_j^2\rangle^{1/2}}$$

and

$$C_4^{ij}(t)=\frac{\langle[\mathbf{r}(t)\times\boldsymbol{\omega}(t)]_i r_j(0)\rangle}{\langle(\mathbf{r}\times\boldsymbol{\omega})_i^2\rangle^{1/2}\langle r_j^2\rangle^{1/2}}$$

exist at all state points. The intensity of the function C_4 is greatest at the critical point, the (3,3) element reaching an intensity of 0.45 (Fig. 4). The time dependence at the other state points is broadly similar to the example in this figure, the intensity falling to a maximum of 0.2 at 1 bar and 293 K and rising to 0.35 at 15 kbar and 1273 K. At 250 kbar and 1043 K the intensity has fallen to 0.12 with a much shorter time dependence. The broad pattern over all the state points is, therefore, opposite to the simple cross-correlation functions of Fig. 1; the intensity is a minimum at high pressures

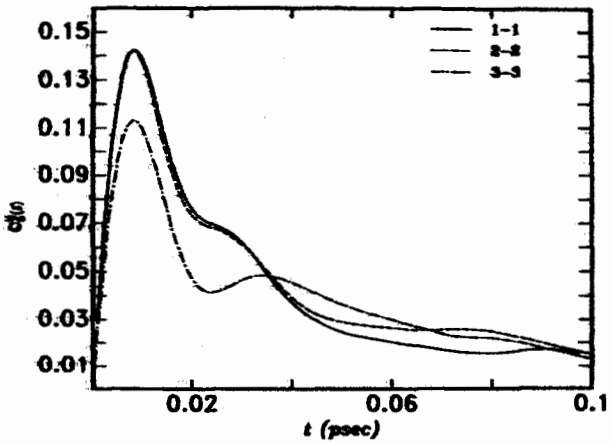

FIG. 5. Example of the diagonal elements of C_4 in the moving frame of reference: liquid water at 250 kbar and 1043 K.

for the higher order CCF and a maximum for the simple CCFs.

The overall pattern of behavior of the higher order moving frame CCF C_4 is similar. In Fig. 5 we illustrate the time dependence at 250 kbar and 1043 K only. This consists of a sharp peak at about 0.01 ps of maximum intensity 0.14. The intensity of this CCF is again a maximum at the critical point.

In the laboratory frame of reference the higher order CCFs:

$$C_5^{ij}(t)=\frac{\langle[\mathbf{v}(t)\times\boldsymbol{\omega}(t)]_i[\mathbf{F}(0)\times\boldsymbol{\omega}(0)]_j\rangle}{\langle(\mathbf{v}\times\boldsymbol{\omega})_i^2\rangle^{1/2}\langle(\mathbf{F}\times\boldsymbol{\omega})_j^2\rangle^{1/2}}$$

and

$$C_6^{ij}(t)=\frac{\langle[\mathbf{v}(t)\times\boldsymbol{\omega}(t)]_i[\mathbf{T}_q(0)\times\mathbf{v}(0)]_j\rangle}{\langle(\mathbf{v}\times\boldsymbol{\omega})_i^2\rangle^{1/2}\langle(\mathbf{T}_q\times\mathbf{v})_j^2\rangle^{1/2}}$$

exist over the whole range of state points. In this case, however, the intensity behavior is remarkably constant up to the kbar range, and there is no maximum intensity at the critical

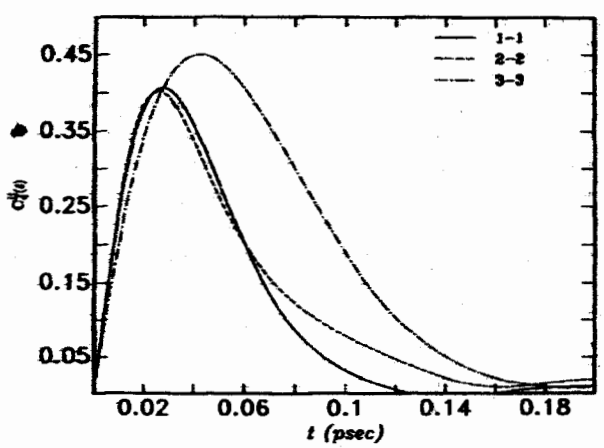

FIG. 4. Example of the diagonal elements of C_4 in the moving frame of reference: liquid water at 221 bar and 674 K (critical point).

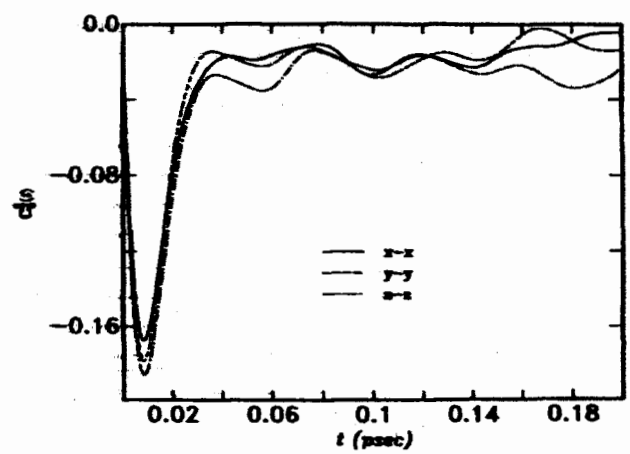

FIG. 6. Example of the diagonal elements of C_5 in the moving frame of reference: liquid water at 15.0 kbar and 1273 K.

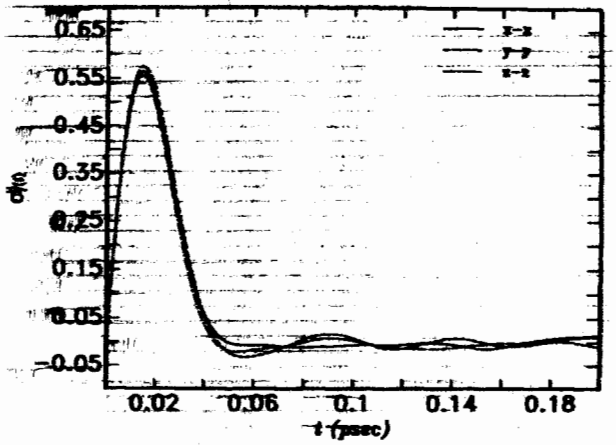

FIG. 7. Example of the diagonal elements of C_t in the moving frame of reference: liquid water at 1.0 bar and 293 K.

point. The function is illustrated in Fig. 6 for 15.0 kbar and 1273 K. The maximum intensity of C_t remains constant at about 0.5 across the complete range of state points and is illustrated in Fig. 7 at 1.0 bar and 293 K.

E. Pair distribution functions

Figure 8 illustrates some oxygen–oxygen pair distribution functions for water splat quenched to 10 K and at the very high density achieved by shock wave compression to 250 kbar and 1043 K. At 10 K the computer simulation results produce three peaks in the range of correlation up to 6.0 Å. In this region the experimental oxygen–oxygen PDF also has three main peaks, but the experimental PDF in amorphous solid ice reflects a more tightly packed structure than that from the computer simulation. The three peaks from the simulation [Fig. 8(a)] are broader and are positioned progressively further out from the origin than their equivalents in the experimentally derived PDF of amorphous solid water. This seems to suggest that the state arrived at in the computer simulation is a very supercooled liquid-like structure. This conclusion is supported by the similarity of the molecular dynamics at room temperature and splat quenched at 10 K. In Fig. 8(b) the oxygen–oxygen PDF at 250 kbar and 1043 K is compared with the equivalent from the same potential at 293 K and 1 bar. It is clear from this figure that the PDF at the high density condition has a fairly pronounced shoulder at about 2.8 Å which is absent at room temperature and pressure. This is reminiscent of the extra structure developed in the splat quenched condition at 10 K.

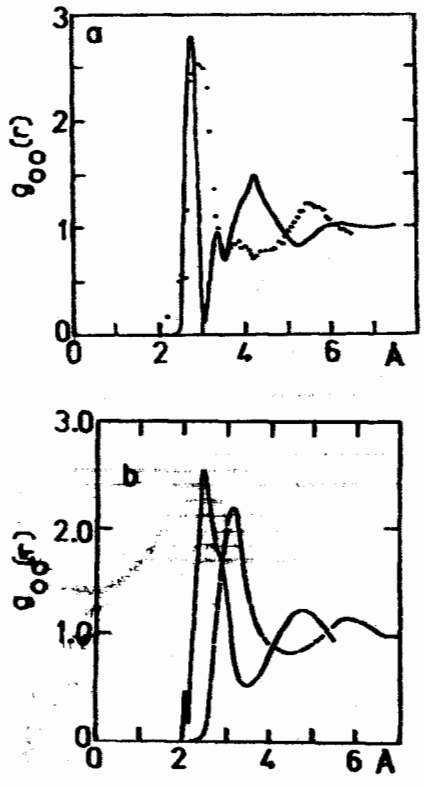

FIG. 8. (a) Oxygen–oxygen pair distribution functions: — Experimental result for amorphous solid ice at 10 K; · · · computer simulation (see the text); (b) comparison of O–O PDFs at 293 K, 1.0 bar (- - -) and 250.0 kbar, 1043 K (—).

V. CONCLUSIONS

Using high quality computer simulations over 6000 time steps on the 1CAP1 system at IBM Kingston the dynamical and structural properties of liquid water have been observed over a broad range of conditions. A simple linked Langevin theory of the rotation–translation dynamics has been developed to account for the coupling function observed in this work at all the simulated state points. This is capable of reproducing the main features of the simulated coupling function. The structural properties of water splat quenched to 10 K have been compared with those experimentally observed in amorphous solid water at this temperature. The simulated structure at this temperature is "looser" and more liquid-like than the observed structure. The model intermolecular pair potential used in this work succeeds in reproducing the observed pressures satisfactorily in the kbar range, but is about twice too high in the 100 kbar range at up to 1043 K.

ACKNOWLEDGMENT

IBM is thanked for the award of a year's Visiting Professorship to M.W.E.

[1] C. W. Burnham, J. R. Holloway, and N. F. Davis, *Thermodynamic Properties of Water to 1,000 C and 10,000 Bars* (Pennsylvania State University, University Park, 1968).
[2] M. H. Price and J. M. Walsh, J. Chem. Phys. 26, 824 (1957).
[3] M. G. Sceats and S. A. Rice, in *Water, A Comprehensive Treatise*, edited by F. Franks (Plenum, New York, 1982), Vol. 7, Chap. 2, p. 83.
[4] C. A. Angell, in Ref. 3, Chap. 1.
[5] A. C. Belch, S. A. Rice, and M. G. Sceats, Chem. Phys. Lett. 77, 455 (1981).
[6] For example, O. C. Bridgeman and E. W. Aldrich, J. Heat Transfer 87, 266 (1965).
[7] M. W. Evans, Phys. Rev. A 34, 2302 (1986); 35, 2989 (1987).
[8] M. W. Evans, J. Chem. Phys. 87, 2257 (1987).
[9] M. W. Evans, J. Chem. Phys. 86, 4096 (1987).
[10] M. W. Evans, Phys. Rev. Lett. 55, 1551 (1985).

[11]Reference 3, pp. 90 ff.
[12]A. H. Narten, C. G. Venkatesh, and S. A. Rice, J. Chem. Phys. 64, 1106 (1976).
[13]G. P. Johari, Philos. Mag. 35, 1077 (1977).
[14]M. Sugisaki, H. Suga, and S. Seki, Bull. Chem. Soc. Jpn. 41, 2591 (1968).
[15]References 4, pp. 16 ff.
[16]M. W. Evans, J. Mol. Liq. 32, 173 (1986).
[17]G. J. Evans, M. W. Evans, P. Mingazzi, C. J. Reid, G. Salvetti, and J. K. Vij, J. Mol. Liq. 34, 285 (1987).
[18]M. W. Evans, J. Mol. Liq. 33, 271 (1987).
[19]G. C. Lie and E. Clementi, J. Chem. Phys. 64, 2314 (1976).
[20]F. H. Stillinger and A. Rahman, J. Chem. Phys. 60, 1545 (1974).
[21]M. W. Evans, G. C. Lie, and E. Clementi, Chem. Phys. Lett. 138, 149 (1987).
[22]G. C. Lie and E. Clementi, Phys. Rev. A. 33, 2679 (1986).
[23]M. D. Morse and S. A. Rice, J. Chem. Phys. 76, 650 (1982).
[24]M. W. Evans, G. J. Evans, W. T. Coffey, and P. Grigolini, *Molecular Dynamics* (Wiley Interscience, New York, 1982).
[25]*Memory Function Approaches to Stochastic Problems in Condensed Matter*, edited by M. W. Evans, P. Grigolini, and G. Pastori-Parravicini, Advances in Chemical Physics Series, Vol. 62 (Wiley Interscience, New York, 1985).
[26]D. W. Condiff and J. S. Dahler, J. Chem. Phys. 44, 3988 (1966).
[27]M. W. Evans, Phys. Rev. A 33, 1903 (1986).
[28]M. W. Evans, Phys. Rev. A 34, 468 (1986).
[29]M. W. Evans, J. Mol. Liq. 31, 213 (1986).
[30]M. W. Evans, J. Mol. Liq. 31, 231 (1986).